Immobilization of lead and copper in aqueous solution and soil using hydroxyapatite derived from flue gas desulphurization gypsum

Yang Liu [a,1], Yubo Yan [a,b,1], Balaji Seshadri [b], Fangjie Qi [b], Yilu Xu [c], Nanthi Bolan [b,*], Fenglian Zheng [d], Xiuyun Sun [a,*], Weiqing Han [a], Lianjun Wang [a,*]

[a] *Jiangsu Key Laboratory of Chemical Pollution Control and Resources Reuse, School of Environmental and Biological Engineering, Nanjing University of Science and Technology, Nanjing 210094, China*
[b] *Global Centre for Environmental Remediation, University of Newcastle, Callaghan, NSW 2308, Australia*
[c] *Future Industries Institute, University of South Australia, Mawson Lakes, SA 5095, Australia*
[d] *China Energy Engineering Group Beijing Electric Power Construction Company, Beijing 100024, China*

A B S T R A C T

Flue gas desulphurization (FGD) gypsum is an abundant waste generated from coal-fired power plants. This study evaluated the potential application of hydroxyapatite (F-HAP) derived from FGD gypsum for immobilization of lead (Pb) and copper (Cu) in water and soil. MINTEQ software was employed to determine the species distribution of Pb(II) and Cu(II) at different solution pH conditions. The factors that affect sorption behavior such as pH effect, sorption kinetics, thermodynamics, and isotherms were investigated using batch tests. Various kinetics and isotherms models were used to fit the obtained data. The experimental results showed that the amount of Pb(II) and Cu(II) adsorbed on F-HAP increased as the pH increased from 2.0 to 6.0, and adsorption was enhanced with the rise in temperature. The predicted maximum adsorption capacities were found to be 1.376 and 0.460 mmol/g for Pb(II) and Cu(II), respectively. The values of mean free energy (E) obtained from Dubinin-Radushkevich (D-R) model implied that the chemical reaction, which was stronger than ion exchange governed the process of Pb(II) adsorption, while the adsorption of Cu(II) was mainly ascribed to ion exchange. XRD analysis revealed that the final solid obtained after Pb(II) immobilization was mainly mixed of pyromorphite and F-HAP, while the final solid acquired after Cu(II) immobilization still consisted of a single phase of F-HAP. On the other hand, application of F-HAP in contaminated soil effectively reduced the leachable and exchangeable Pb and Cu, reflecting that F-HAP is a potential material for remediating environmental pollution with Pb and Cu. This study realized the potential of a modified geochemical waste material towards remediation of metal contaminated soils, providing very useful and valuable information for other similar solid wastes, such as paper sludge and phosphogypsum.

1. Introduction

With rapid development of industrialization, toxic heavy metals such as lead (Pb) and copper (Cu) are ubiquitous in water and soil, posing serious threats to plants, animals and even human beings. Pb has been widely used for different purposes such as battery manufacturing, paints, ceramics, metal plating, ammunition (Ahmad et al., 2012; Shahat et al., 2015). The accumulation of Pb or its compounds in living organisms can damage the central nervous system, brain, kidney, and circulatory system, which may cause severe poisoning that may lead to intellectual disability, anemia, mental deficiency or cancer (Huang and

Pan, 2016; Ma et al., 2015). Cu has been widely used in processing of ores and oil, paper and paper board mills, manufacture of ceramics, electroplating, glass making, production of fertilizers, etc. (Dean et al., 1972; Gandhi and Meenakshi, 2011). Exposure to higher concentrations (>5 mg Cu/L) has been linked to serious kidney failure and liver diseases (Pawar et al., 2016). Hence, developing technologies to efficiently immobilize Pb and Cu thereby reducing their mobility and availability in environment are urgently and universally required.

Recently, utilization of phosphate for adsorption and immobilization of heavy metal ions has been considered as a cost-effective and environmentally positive technology for treating heavy-metal contaminated water and soil (Cao et al., 2004; Liu and Zhao, 2007; Seshadri et al., 2016). Liang et al. (2011) found that hydroxyapatite derived from the porous glass strongly adsorbed Pb(II) and Cu(II). Matusik et al. (2008) compared the effectiveness of different phosphate compounds (K_2HPO_4, $NH_4H_2PO_4$ and "*Polifoska 15*" fertilizer) on Cd(II) immobilization. The

results showed that all used forms of phosphates presented >99% reduction for Cd(II) removal from aqueous solution, and the process was mainly influenced by pH condition rather than source of phosphates. Yang and Mosby (2006) demonstrated that the application of H_3PO_4 significantly reduced the risk of Pb mobility in smelter-contaminated urban soil. Hamon et al. (2002) assessed the remediation effect of $CaCO_3$, KH_2PO_4, redmud, and a kaolin byproduct on Cd and Zn in a polluted soil. The results showed that immobilization of both Cd and Zn was greatest in KH_2PO_4 treated soil, and this treatment was also found to be resistant to soil acidification. Mignardi et al. (2012) used synthetic hydroxyapatite and natural phosphate rock to immobilize Cd, Cu, Pb, and Zn in mine waste soils. The results showed that both materials effectively reduced the heavy metal water solubility generally by about 84–99%, and synthetic hydroxyapatite was slightly superior to natural phosphate rock for immobilizing heavy metals. Ogawa et al. (2015) used hydroxyapatite and ferrihydrite both individually and in combination to immobilize Pb in shooting range soil and observed marked increase in Pb immobilization for the combined treatment. However, the stability of immobilized Pb was similar for hydroxyapatite alone and the combined treatment. Although soluble phosphate (e.g., K_2HPO_4, $NH_4H_2PO_4$) was highly effective in immobilization of heavy metals, excess phosphate in soil is still a potential risk to the environment (Cao et al., 2004; Jiang et al., 2012). Hydroxyapatite (HAP, $Ca_{10}(PO_4)_6(OH)_2$) is a less soluble phosphate, furthermore, it is environmentally friendly and possesses high stability under reducing and oxidizing conditions, which would be an ideal amendment for the immobilization of heavy metals.

In order to reduce the production costs of HAP, many scientists attempted to develop low-cost source of calcium to replace expensive reagents. Sanosh et al. (2009) synthesized nano-HAP powder from biowaste chicken eggshells. Piccirillo et al. (2013) immobilized the special bacterial strains on fish bones based HAP for water treatment. Muhammad et al. (2016) extracted HAP from the waste fish scales with the yield of ~32%. However, these attempts are based on biowastes and the research involving industrial by-products is limited.

In our previous work, flue gas desulphurization (FGD) gypsum, a second largest solid waste in coal-fired power plants has been successfully transformed to hydroxyapatite (F-HAP) (Yan et al., 2014). The overall goal of this study is to evaluate the feasibility of using F-HAP to immobilize Pb(II) and Cu(II) in aqueous solution and soil. The specific objectives are to: (1) investigate the adsorption behavior of Pb(II) and Cu(II) in aqueous solution based on pH impact, sorption kinetics, thermodynamics, and isotherms; (2) compare the leachability of Pb and Cu in unamended and amended soils via toxicity characteristics leaching procedure (TCLP) method; and (3) study the effect of F-HAP addition on the distribution of Pb and Cu in soil.

2. Materials and methods

2.1. Materials and soil collection

Chemical reagents used in this work are all analytical grade. FGD gypsum samples were collected from a coal-fired power plant in Nanjing, China. F-HAP with a Ca/P molar ratio of 5:3 was prepared by the stoichiometric reaction between FGD gypsum and KH_2PO_4 solution as described by Yan et al. (2014) with a minor modification.

The stock solutions of Pb(II) and Cu(II) were prepared by dissolving $Pb(NO_3)_2$ and $Cu(NO_3)_2$ in Milli-Q water, respectively. The required concentrations in adsorption experiments were prepared by diluting the stock solutions. KNO_3 (0.01 M) was used to maintain the ionic strength of all solutions. NaOH (0.1 M) and HNO_3 (0.1 M) were used to adjust the pH of all solutions.

Soil samples contaminated with Pb and Cu were collected from a small firing range in Nanjing, China at a depth of 0–20 cm. The samples were air-dried and sieved through a 10-mesh sieve to remove the large bullet fragments and provide homogeneous fractions. The total Pb and Cu concentrations based on extraction by the mixed concentrated acid

(HNO_3-$HClO_4$-HF) (Lu, 1999) were approximately 3715 and 284 mg/kg, respectively.

2.2. Adsorption experiments

Batch experiments were carried out by mixing 0.1 g F-HAP with 100 mL diluted stock solutions of Pb or Cu in conical flasks, and the mixtures were shaken in an air bath oscillator at a speed of 200 rpm. After adsorption, the mixtures were filtered through 0.22 μm membrane filter for analysis of the residual metals concentration by Inductively Coupled Plasma Optical Emission Spectrometer (ICP-OES, Optima 7000DV). The adsorption capacity (q_e, mmol/g) were calculated from the following equations:

$$q_e = \frac{(C_0 - C_e)V}{m} \tag{1}$$

where C_0 and C_e (mmol/L) are initial and equilibrium concentrations of adsorbate, respectively, V (L) is the volume of solutions, and m (g) is the dosage of adsorbent.

The experiments on pH impact were performed at 25 °C, the pH values of the solutions with 1.0 mmol/L concentration of Pb and Cu solutions were adjusted to 2.0, 3.0, 4.0, 5.0, and 6.0. Kinetic experiments were carried out at different periods (0, 5, 10, 15, 30, 45, 60, 90, 120, 150, 180, 240, and 300 min) for three temperatures (25, 35 and 45 °C) using 1.0 mmol/L concentration of Pb and Cu solutions. Adsorption isotherms were obtained using various Pb (0.5, 1.0, 1.5, 2.0, and 3.0 mmol Pb/L) or Cu (0.1, 0.5, 1.0, 1.5, and 2.0 mmol Cu/L) concentrations.

2.3. Theories

2.3.1. Kinetic models

Two well-known kinetic models, pseudo-first order (Ho, 2004) and pseudo-second order models (Ho, 2006) were usually used to study the controlling mechanism of the adsorption process such as mass transfer, diffusion control or chemical reaction. Their non-linear forms are expressed as:

$$\text{Pseudo-first order equation}: \quad q_t = q_e\left(1 - e^{-k_1 t}\right) \tag{2}$$

$$\text{Pseudo-second order equation}: \quad q_t = \frac{k_2 q_e^2 t}{1 + k_2 q_e t} \tag{3}$$

where q_e and q_t (mmol/g) represent the amount of adsorbate adsorbed at equilibrium and at time t, k_1 (min^{-1}) and k_2 (g/(mmol min)) are the rate constants for the pseudo-first order and pseudo-second order models, respectively.

In addition, when $t \rightarrow 0$, the initial adsorption rate, h (mmol/(g min)), can be calculated by:

$$h = k_2 q_e^2 \tag{4}$$

2.3.2. Thermodynamic studies

The thermodynamic parameters including Gibbs free energy change ($\Delta G°$, kJ/mol), enthalpy change ($\Delta H°$, kJ/mol) and entropy change ($\Delta S°$, kJ/mol/K) were determined by (Wang et al., 2012):

$$\Delta G° = -RT \ln K \tag{5}$$

$$\ln K = \frac{\Delta S°}{R} - \frac{\Delta H°}{RT} \tag{6}$$

where K is the adsorption equilibrium constant, R is the ideal gas constant, 8.314 J/mol/K, and T (K) is the temperature.

2.3.3. Isotherm models

[Langmuir (1918)](#) and [Freundlich (1906)](#) isotherm models are widely used to describe the adsorption characteristics of adsorbent surface such as homogeneous reaction or heterogeneous reaction. Their non-linear forms can be written as:

$$\text{Langmuir equation}: \quad \frac{C_e}{q_e} = \frac{C_e}{q_{max}} + \frac{1}{bq_{max}} \tag{7}$$

$$\text{Freundlich equation}: \quad \log q_e = \log K_F + \frac{1}{n} \log C_e \tag{8}$$

where C_e (mmol/L) is the equilibrium concentration of adsorbate, q_e (mmol/g) is the amount of adsorbate adsorbed under equilibrium, q_{max} (mmol/g) is the maximum adsorption capacity, b (L/mmol) is a Langmuir constant related to the affinity of the binding sites and energy of adsorption, and K_F and n are Freundlich constants with n giving an indication of how favorable the adsorption process and K_F (mmol/g) related to the bonding energy.

Dubinin-Radushkevich (D-R) model ([Dubinin, 1960](#)) was employed to further study the mechanism of Pb(II) and Cu(II) on F-HAP. Its linear forms can be represented by:

$$\ln q_e = \ln q_m - \beta \varepsilon^2 \tag{9}$$

$$\varepsilon = RT \ln \left(1 + \frac{1}{C_e} \right) \tag{10}$$

$$E = \frac{1}{\sqrt{2\beta}} \tag{11}$$

where q_m (mmol/g) is the theoretical saturation adsorption capacity, β (mol^2/J^2) is a constant correlated with the mean free energy of adsorption, ε is the Polanyi potential, and E (mol^2/kJ^2) is the mean free energy of adsorption per molecule of the adsorbate when transferred to the surface of the solid from infinity in the solution.

2.4. Incubation experiments

100 g portions of metal contaminated soil samples were mixed thoroughly with F-HAP at ratio of 0, 1, 3.0, 5.0, 7.0, and 10% (w/w) in plastic cups. The sealed cups were wetted with Milli-Q water to 60% of water holding capacity, and then incubated at the room temperature (27 ± 2 °C) for 4 weeks. During the period of incubation, the cups were weighed every week and water was added to maintain constant moisture content.

2.5. Leachability of Pb(II) and Cu(II)

The potential leachability of heavy metals in treated soil samples was measured according to the toxicity characteristics leaching procedure (TCLP) method ([USEPA, 1994](#)). 2.00 g of each F-HAP treated and untreated soil samples were added to 40 mL of fresh TCLP leaching fluid (acetic acid solution with pH 2.88 ± 0.05) and the centrifuge tubes were then shaken at a speed of 30 rpm and 25 °C for 18 h.

2.6. Redistribution of Pb(II) and Cu(II)

The distribution of heavy metals in treated soil samples was determined according to the sequential extraction method ([Tessier et al., 1979](#)), which divides heavy metals into five different forms: (1) exchangeable form (EX): extracted by 1.0 M MgCl$_2$ at pH 7.0 for 1 h, (2) carbonate-bound form (CB): extracted by 1.0 M NaOAc/HOAc at pH 5.0 for 5 h, (3) Fe/Mn oxide-bound form (OX): extracted by 0.04 M NH$_2$OH·HCl in 25% (vol.%) HOAc solution for 6 h, (4) organic-bound form (OR): extracted firstly by 0.02 M HNO$_3$ in 30% (wt.%) H$_2$O$_2$ solution for 2 h, then by 30% (wt.%) H$_2$O$_2$ solution for 2 h, and finally by 3.2 M

NH$_4$OAc in 20% HNO$_3$ solution (vol.%) for 0.5 h, and (5) residual form (RES): digested by HNO$_3$-HClO$_4$-HF.

3. Results and discussion

3.1. Effect of pH

The adsorption of metal ions from aqueous solution was highly dependent on the solution pH as it can impact both the species distribution of metal ions and the surface charge of the adsorbents. To avoid the interference of metal hydroxides species on adsorption, the acidic pH range of 2.0–6.0 was chosen for study of pH impact. Modeling analysis by the Visual MINTEQ software also confirms that Pb^{2+} and Cu^{2+} are the dominant species in this pH range ([Fig. 1](#)). As shown in [Fig. 2](#), it was apparent that the adsorption capacities (q_e) of both Pb(II) and Cu(II) increased sharply when the pH was lower than 5.0, and then the q_e increased slightly as the pH increased from 5.0 to 6.0. The removal efficiency of Pb(II) and Cu(II) was 80.2 and 35.9% at pH 6.0, and only 30.9 and 10.9% at pH 2.0, respectively. There are two possible reasons for the variation in the metal adsorption capacity of F-HAP in this pH range. Firstly, the partial dissolution of F-HAP in acidic medium resulted in the reduction of adsorption sites. On the other hand, lower pH condition destroyed the embedded calcium triangles in F-HAP crystal structure, which induced the protonation on the surface of F-HAP ([Zhang et al., 2012](#)). The repulsive forces between positively charged surface and Pb^{2+}/Cu^{2+} hinder the diffusion of Pb^{2+}/Cu^{2+} to F-HAP surface. The pH 5.0 was chosen for following studies.
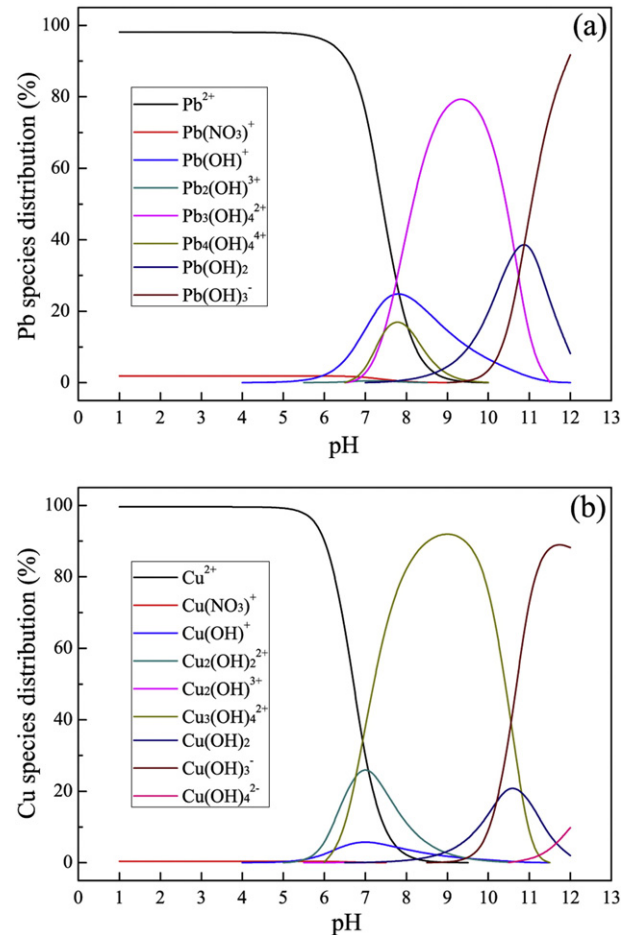

Fig. 1. Species distribution of Pb (a), and Cu (b) over wide pH ranges from 1.0 to 12, as calculated by the Visual MINTEQ software (ionic strength: 0.01 mol/L KNO$_3$; temperature: 25 °C).
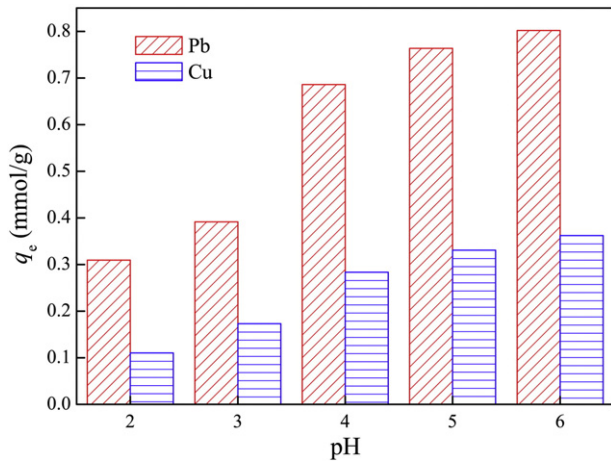
Fig. 2. Effect of pH condition on the adsorption of Pb(II) and Cu(II) by F-HAP.

3.2. Kinetic studies

Fig. 3 shows the kinetic adsorption behavior of metal ions by F-HAP at different temperatures. For both Pb(II) and Cu(II), the adsorption capacity increased rapidly in the beginning of the process, and then slowed down until a pseudo equilibrium was reached. Moreover, the adsorption ability of F-HAP was enhanced significantly as rising the temperature from 25 to 45 °C, i.e., the removal efficiency increased from 77.7 to 99.8% for Pb(II) and 37.7 to 56.5% for Cu(II), indicating the available active sites on the surface of F-HAP increased with the temperature.

The curves of non-linear fitting along with the experimental data are plotted in Fig. 3, and the corresponding parameters are listed in Table 1. It can be observed that the correlation coefficients (R^2) of pseudo-second order kinetic model were all higher than those for pseudo-first order model for both metal ions. Meanwhile, the theoretical adsorption capacities (q_e) calculated from Eq. (3) matched the experimental observations well at all studied temperatures. The results indicated the better applicability of pseudo- second order kinetic model for both Pb(II)

and Cu(II). This also suggested that the overall rates of Pb(II) and Cu(II) sorption are both controlled by the chemisorption procedure (Yang et al., 2014). Additionally, the initial adsorption rates followed $h_{45} > h_{35} > h_{25}$ for Pb(II) (0.082, 0.085, and 0.106 mmol/(g min) at 25, 35, and 45 °C, respectively) and Cu(II) (0.032, 0.039, and 0.041 mmol/(g min) at 25, 35, and 45 °C, respectively), which was in good agreement with the trend as shown in Fig. 3. Furthermore, adsorption of Pb(II) on F-HAP was over 2.0 times faster than Cu(II) at the initial period, implying a stronger interaction between F-HAP and Pb(II).

3.3. Thermodynamic studies

It is well-known that the thermodynamic parameters can be used to assess the orientation and feasibility of the physicochemical adsorptive reaction (Li et al., 2005). All the parameters are presented in Table 2. It was noted that for all conditions $\Delta G°$ became more negative as temperature raised, indicating the feasibility and spontaneous adsorption of Pb(II) and Cu(II) on F-HAP. The positive values of $\Delta H°$ suggested the endothermic adsorption process, which was supported by increased adsorption of metals at high temperature. The positive $\Delta S°$ values stated that the randomness increased at the solid-solution interface during the adsorption process, suggesting that some structural exchange may occur among the active sites of F-HAP and the ions (Rehman et al., 2006).

3.4. Isotherm studies

The adsorption of Pb(II) and Cu(II) on F-HAP as a function of their concentrations was shown in Fig. 4a. It was found that the equilibrium adsorption capacity of F-HAP for Pb(II) and Cu(II) both increased with increasing initial concentrations. This is probably due to a high driving force for mass transfer in high metal ions concentration. It was also observed that Pb(II) uptake in entire process was higher than Cu(II), which also implied the relatively high affinity between Pb(II) and F-HAP.

As shown in Fig. 4 (b–d), Langmuir, Freundlich and Dubinin-Radushkevich (D-R) models were used to describe the adsorption behavior at equilibrium. The obtained parameters of all models are summarized in Table 3. By comparing the correlation coefficients (R^2), it could be deduced that the experimental equilibrium data of Pb(II)
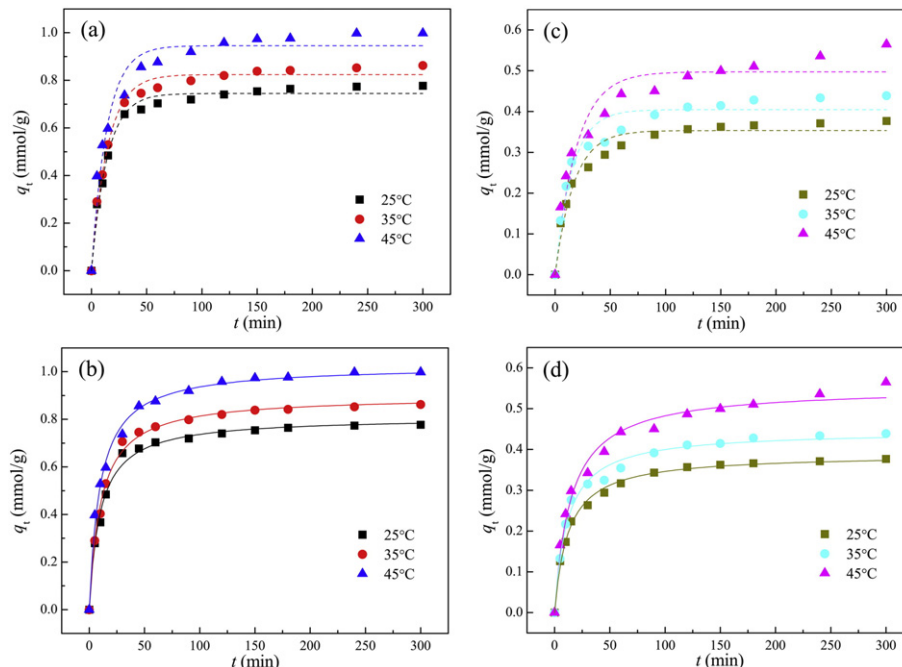

Fig. 3. The plots of pseudo-first order model for Pb(II) (a) and Cu(II) (c), and the plots of pseudo-second order model for Pb(II) (b) and Cu(II) (d).

Table 1
Pseudo-first order and pseudo-second order kinetic parameters for the adsorption of Pb(II) and Cu(II) on F-HAP.

	$q_{e,exp}$ (mmol/g)	Pseudo-first order			Pseudo-second order		
		k_1 (min^{-1})	$q_{e,cal}$ (mmol/g)	R^2	k_2 (g/mmol min)	$q_{e,cal}$ (mmol/g)	R^2
Pb(II)							
25 °C	0.777	0.071	0.744	0.987	0.125	0.809	0.993
35 °C	0.863	0.068	0.824	0.988	0.106	0.898	0.996
45 °C	0.998	0.072	0.946	0.961	0.101	1.026	0.995
Cu(II)							
25 °C	0.377	0.059	0.353	0.961	0.212	0.388	0.996
35 °C	0.439	0.065	0.405	0.946	0.196	0.446	0.988
45 °C	0.565	0.051	0.497	0.934	0.134	0.552	0.984

Table 2
Thermodynamic parameters for the adsorption of Pb(II) and Cu(II) on F-HAP.

	T (°C)	$\Delta G°$ (kJ/mol)	$\Delta H°$ (kJ/mol)	$\Delta S°$ (kJ/mol/K)
Pb(II)	25	−12.59	15.58	0.078
	35	−13.28		
	45	−14.09		
Cu(II)	25	−7.87	9.85	0.075
	35	−8.50		
	45	−9.44		

sorption was best fit to the Langmuir model, while the Freundlich model was best suitable for Cu(II) sorption. This suggests the homogeneous reaction on the surface for Pb(II) sorption and heterogeneous reaction for Cu(II) sorption. According to the q_{max} parameter, the preference of sorption exhibited by F-HAP was more pronounced for Pb(II) than for Cu(II). This could be attributed to (1) Pb(II) (1.32 Å) possesses larger ionic radii than Cu(II) (0.72 Å), which more likely leads to the incorporation of Pb(II) into the F-HAP structure, and (2) Pb(II) (2.33) is more electronegative than Cu(II) (2.00), which is conducive to the electrostatic and inner sphere surface complexation reactions (LeGeroes and LeGeroes, 1984; Liu et al., 2008; Zhang et al., 2010). In comparison with other adsorbents (Table 4), the relatively high q_{max}s in this study implied that F-

HAP had a significant potential for removal of Pb(II)/Cu(II) in practical cases. The Langmuir constant, b is often used to calculate the dimensionless separation factor, R_L ($R_L = 1/(1 + bC_0)$), which can assess the favorability and affinity of adsorption. The adsorption is unfavorable when $R_L > 1$; it is linear when $R_L = 1$; it is favorable when it is $0 < R_L < 1$; and it is irreversible when $R_L = 0$ (Meitei and Prasad, 2014). Here, all R_L values calculated were between 0 and 1 (0.029–0.152 for Pb(II) and 0.050–0.513 for Cu(II)), indicating that F-HAP was favorable adsorbent for Pb(II) and Cu(II) adsorption. Also, the R_L values of Pb(II) were lower than those for Cu(II), implying much higher affinity between Pb(II) and F-HAP. In addition, the 1/n values calculated from Freundlich equations were both within the range of 0–1, suggesting that the conditions were favorable for adsorption in two cases.

The E value calculated from D-R equations is useful for distinguishing the adsorption as physical or chemical process. When E value lies between 1 and 8 kJ/mol, indicating physical adsorption, its value in range of 8–16 kJ/mol is an indicator of ion exchange, while if its value is between 20 and 40 kJ/mol, it indicates chemical adsorption (Chen et al., 2010; Hamayun et al., 2014). In this study, 27.54 kJ/mol for Pb(II) sorption indicated a strong chemical reaction. On the other hand, 9.26 kJ/mol for Cu(II) indicated that the ion exchange mechanism more likely governed Cu(II) adsorption. Comparing with the X-ray diffraction (XRD) patterns displayed in Fig. 5, it was evident that no structural changes of F-HAP after Cu(II) adsorption, while a mixed phase of
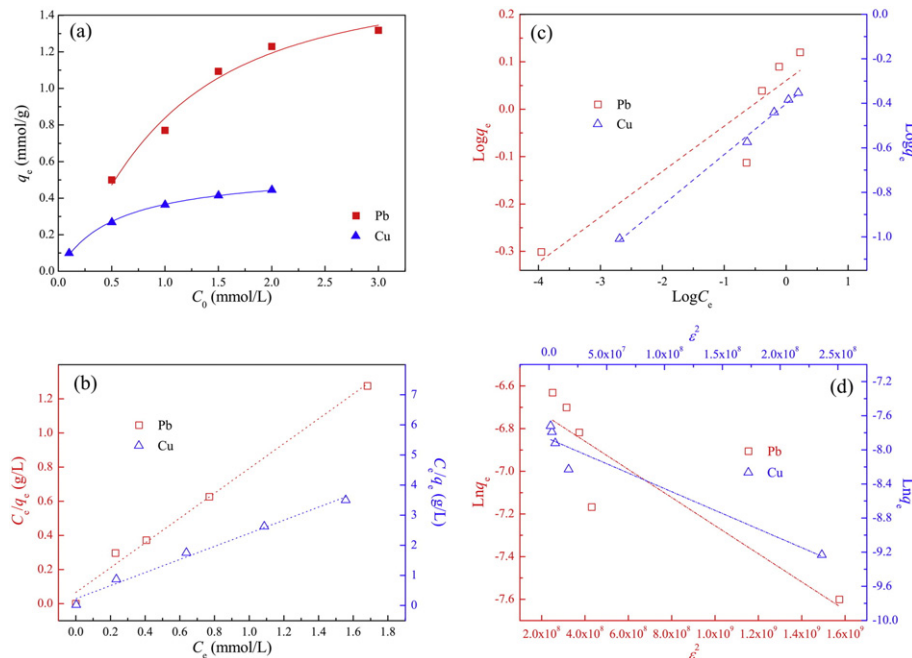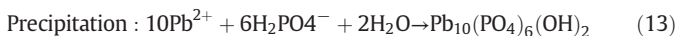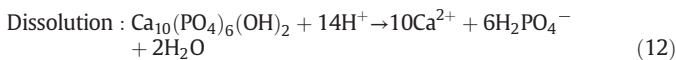

Fig. 4. (a) Effect of initial concentrations of Pb(II) and Cu(II) on their uptake by F-HAP, (b) Langmuir isotherm plots, (c) Freundlich isotherm plots, and (d) D-R isotherm plots.

Table 3
Isotherm parameters for the adsorption of Pb(II) and Cu(II) on F-HAP at 25 °C.

Langmuir			
	q_{max} (mmol/g)	b (L/g)	R^2
Pb(II)	1.376	11.13	0.991
Cu(II)	0.460	9.48	0.987
Freundlich			
	K_F (L/g)	1/n	R^2
Pb(II)	1.149	0.096	0.868
Cu(II)	0.397	0.228	0.997
D-R			
	q_m (mmol/g)	E (kJ/mol)	R^2
Pb(II)	1.367	27.54	0.827
Cu(II)	0.381	9.26	0.934

HAP and pyromorphite ($Pb_{10}(PO_4)_6(OH)_2$, $K_{sp} = 10^{-76.8}$) was detected after Pb(II) adsorption.

Much work has also confirmed that the principal mechanism responsible for the adsorption of Pb(II) by HAP is the dissolution of HAP followed by precipitation of pyromorphite, which is a more stable phase than HAP itself (Hafsteinsdóttir et al., 2015; Jang et al., 2008; Suzuki et al., 1984; Vila et al., 2012). The reactions can be described by the following equations:

$$\text{Dissolution}: Ca_{10}(PO_4)_6(OH)_2 + 14H^+ \rightarrow 10Ca^{2+} + 6H_2PO_4^- + 2H_2O \tag{12}$$

$$\text{Precipitation}: 10Pb^{2+} + 6H_2PO4^- + 2H_2O \rightarrow Pb_{10}(PO_4)_6(OH)_2 \tag{13}$$

However, adsorption of Cu(II) on the HAP surface followed by replacement of Ca(II) is primarily attributed to the adsorption of Cu(II) by HAP (Gandhi and Meenakshi, 2011; Kim et al., 2009; Liang et al., 2011), which can be described by:

$$Ca_{10}(PO_4)_6(OH)_2 + xCu^{2+} \rightarrow Ca_{10-x}Cu_x(PO_4)_6(OH)_2 + xCa^{2+} \tag{14}$$
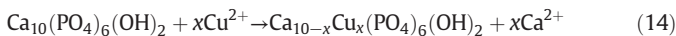
3.5. Leachability

The effect of F-HAP on the TCLP-extractable Pb and Cu in the studied soil is shown in Fig. 6. The data exhibits that the TCLP-extractable concentrations in unamended soil were 117.5 and 30.88 mg/L for Pb and Cu, respectively, which exceeded the standard level set by USEPA (5 and 15 mg/L for Pb and Cu, respectively). Pb and Cu concentrations in TCLP extracts were significantly reduced in the F-HAP treated soil

Table 4
Comparison of adsorption capacities (q_{max}) of various adsorbents for Pb(II) and Cu(II) adsorption.

| Metals	Adsorbent	q_{max} (mmol/g)	Reference
Pb(II)	F-HAP	285	This study
	Modified orange peel	15.27	Lasheen et al. (2012)
	Dairy manure compost	95.3	Zhang (2011)
	Xanthate-modified magnetic chitosan	76.9	Zhu et al. (2012)
	PS-EDTA resin	32.1	Wang et al. (2010)
	Functionalized lignin	123	Yan and Li (2016)
Cd(II)	F-HAP	29.2	This study
	Modified orange peel	73.53	Lasheen et al. (2012)
	Dairy manure compost	27.2	Zhang (2011)
	Modified poplar tree sawdust	6.92	Šćiban et al. (2006)
	Natural kaolinite clay	1.22	Jiang et al. (2010)
	Biochar	3.68–5.56	Guo et al. (2014)
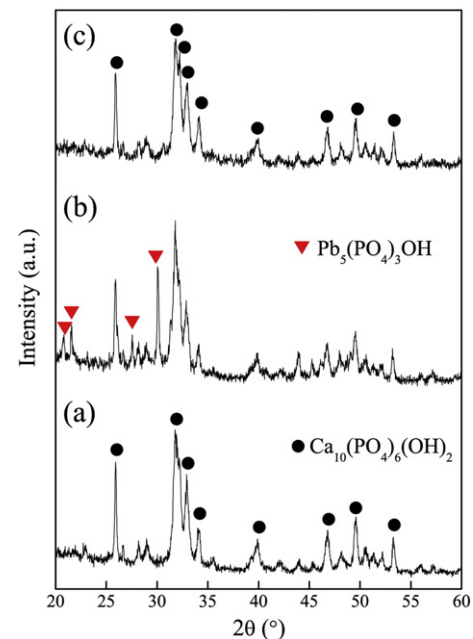
Fig. 5. XRD patterns of F-HAP before and after heavy metal immobilization: (a) F-HAP, (b) Pb, and (c) Cu.

samples and the reduction enhanced with the increase of the F-HAP application rate. However, application of F-HAP reduced the TCLP-extractable Pb concentration more effectively than that of Cu. Specifically, the
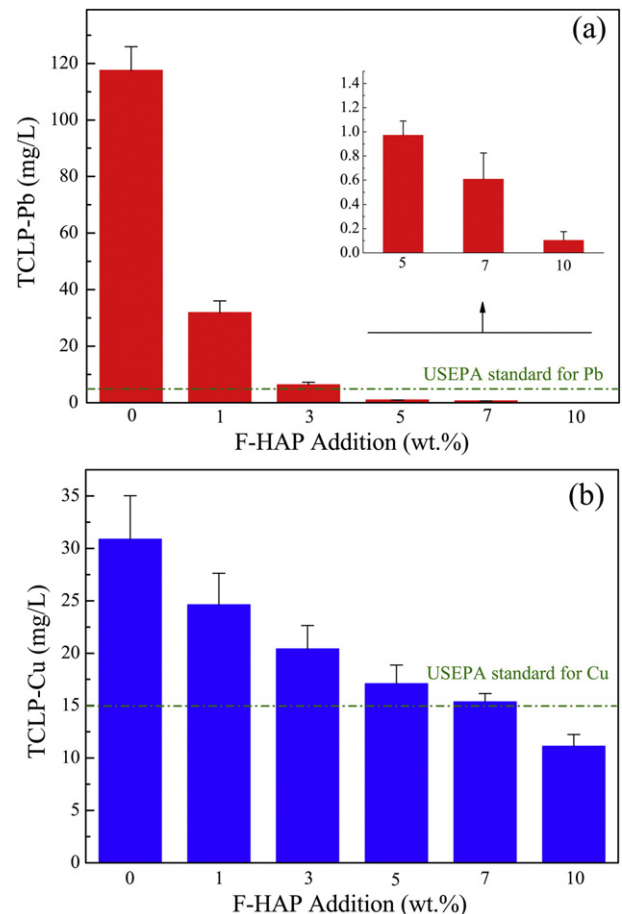

Fig. 6. TCLP-extractable Pb (a) and Cu (b) of the unamended and amended soil with F-HAP.

TCLP-extractable Pb concentration in soil amended with 5% F-HAP reduced below the USEPA standard level of 5 mg/L (Fig. 6a). On the other hand, the applications of >10% F-HAP reduced the TCLP-extractable Cu concentration below the USEPA standard level of 15 mg/L (Fig. 6b). Thus, it can be deduced that the easily available Pb and Cu forms were transformed to more stable forms with the addition of F-HAP.

3.6. Redistribution

The results reflecting the effect of F-HAP addition on the redistribution of Pb and Cu in studied soil are shown in Fig. 7. Initially, the most predominant Pb fraction was CB, accounting for 55.9% of the total Pb, while Cu was primarily associated with OX (43.1%). As the rate of application of F-HAP increased, the distribution of Pb and Cu fractions were notably altered. Specially, the EX percentages of Pb and Cu decreased from 8.35 (0% addition) to 0.02% (10% addition) for Pb and 7.83 (0% addition) to 0.39% (10% addition) for Cu. Similarly, the CB percentages decreased from 55.9 (0% addition) to 9.41% (10% addition) and 39.9 (0% addition) to 25.4% (10% addition) for Pb and Cu, respectively. Within the same time period, the RES percentages increased from 3.04 (0% addition) to 84.5% (10% addition) for Pb and 1.61 (0% addition) to 15.1% (10% addition) for Cu. This indicated that F-HAP could convert the mobile soil bound Pb and Cu to the stable fractions, reducing or eliminating risk to humans and the environment. Moreover, a significant reduction was observed in OX fraction for Pb immobilization (Fig. 7a), whereas, a slight increase was observed in case of Cu (Fig. 7b). This indicated the greater immobilization performance that F-HAP exhibited on Pb compared to Cu, which was consistent with the phenomenon that observed from adsorption tests. A study by Ogawa et al. (2015) using

hydroxyapatite individually and in combination with ferrihydrite showed similar distribution of Pb fractions except for the OX fraction which showed an increase compared to the results shown in this study. This may be attributed to the influence of ferrihydrite on the OX fraction.

4. Conclusions

F-HAP derived from FGD gypsum has proved to be favorable for adsorption of both Pb(II) and Cu(II). The results of kinetic modeling indicated that the systems studied followed the pseudo-second order model more than the pseudo-first order model at all temperatures, implying that the rate-controlling step for immobilization of Pb(II) and Cu(II) was a chemical process. The thermodynamic study indicated that the adsorption of Pb(II) and Cu(II) was spontaneous and endothermic in nature. The isotherm data of Pb(II) adsorption agreed well with Langmuir model, while the Freundlich model was appropriate for Cu(II) adsorption. XRD analysis confirmed that the partial dissolution of F-HAP and re-precipitation of pyromorphite was the main mechanism in adsorption of Pb(II), while the ion exchange was primarily contributed to adsorb Cu(II). The addition of F-HAP to a firing range soil resulted in a significant reduction in the amount of TCLP extractable Pb and Cu, and the satisfying leachability was achieved on 5 wt.% addition for Pb and 10 wt.% addition for Cu. Moreover, sequential extraction analysis indicated that the addition of F-HAP significantly transferred the bioavailable fractions to residual fraction, especially for Pb.

Fig. 7. The effect of F-HAP addition on the fractions of Pb (a) and Cu (b) in soil.

References

Ahmad, M., Hashimoto, Y., Moon, D.H., Lee, S.S., Ok, Y.S., 2012. Immobilization of lead in a Korean military shooting range soil using eggshell waste: an integrated mechanistic approach. J. Hazard. Mater. 209/210, 392–401.

Cao, X., Ma, L.Q., Rhue, D.R., Appel, C.S., 2004. Mechanisms of lead, copper, and zinc retention by phosphate rock. Environ. Pollut. 131, 435–444.

Chen, H., Zhao, J., Dai, G., Wu, J., Yan, H., 2010. Adsorption characteristics of Pb(II) from aqueous solution onto a natural biosorbent, fallen Cinnamomum camphora leaves. Desalination 262, 174–182.

Dean, J.C., Bosqui, F.L., Lanovette, K.H., 1972. Removing heavy metals from waste water. Environ. Sci. Technol. 6, 509–518.

Dubinin, M.M., 1960. The potential theory of adsorption of gases and vapors for adsorbents with energetically non-uniform surface. Chem. Rev. 60, 235–241.

Freundlich, H.M.F., 1906. Over the adsorption in solution. J. Phys. Chem. 57, 385–470.

Gandhi, M.R., Meenakshi, G.N.K.S., 2011. Removal of copper(II) using chitin/chitosan nano-hydroxyapatite composite. Int. J. Biol. Macromol. 48, 119–124.

Guo, Y., Tang, W., Wu, J., Huang, Z., Dai, J., 2014. Mechanism of Cu(II) adsorption inhibition on biochar by its aging process. J. Environ. Sci. 26, 2123–2130.

Hafsteinsdóttir, E.G., Camenzuli, D., Rocavert, A.L., Walworth, J., Gore, D.B., 2015. Chemical immobilization of metals and metalloids by phosphates. Appl. Geochem. 59, 47–62.

Hamayun, M., Mahmood, T., Naeem, A., Muska, M., Din, S.U., Waseem, M., 2014. Equilibrium and kinetics studies of arsenate adsorption by FePO₄. Chemosphere 99, 207–215.

Hamon, R.E., McLaughlin, M.J., Cozens, G., 2002. Mechanisms of attenuation of metal availability in in situ remediation treatments. Environ. Sci. Technol. 36, 3991–3996.

Ho, Y.S., 2004. Citation review of Lagergren kinetic rate equation on adsorption reaction. Scientometrics 59, 171–177.

Ho, Y.S., 2006. Review of second order models for adsorption systems. J. Hazard. Mater. 136, 681–689.

Huang, X., Pan, M., 2016. The highly efficient adsorption of Pb(II) on graphene oxides: a process combined by batch experiments and modeling techniques. J. Mol. Liq. 215, 410–416.

Jang, S.H., Min, B.G., J, Y.G., Lyoo, W.S., Lee, S.C., 2008. Removal of lead ions in aqueous solution by hydroxyapatite/polyurethane composite foams. J. Hazard. Mater. 152, 1285–1292.

Jiang, M., Jin, X., Lu, X., Chen, Z., 2010. Adsorption of Pb(II), Cd(II), Ni(II) and Cu(II) onto natural kaolinite clay. Desalination 252, 33–39.

Jiang, G.J., Liu, Y.H., Huang, L., Fu, Q.L., Deng, Y.J., Hu, H.Q., 2012. Mechanism of lead immobilization by oxalic acid-activated phosphate rocks. J. Environ. Sci. 24, 919–925.

Kim, W.G., Kim, M.N., Lee, S.M., Yang, J.K., 2009. Removal of Cu(II) with hydroxyapatite (animal bone) as an inorganic ion exchanger. Desalin. Water Treat. 4, 269–273.
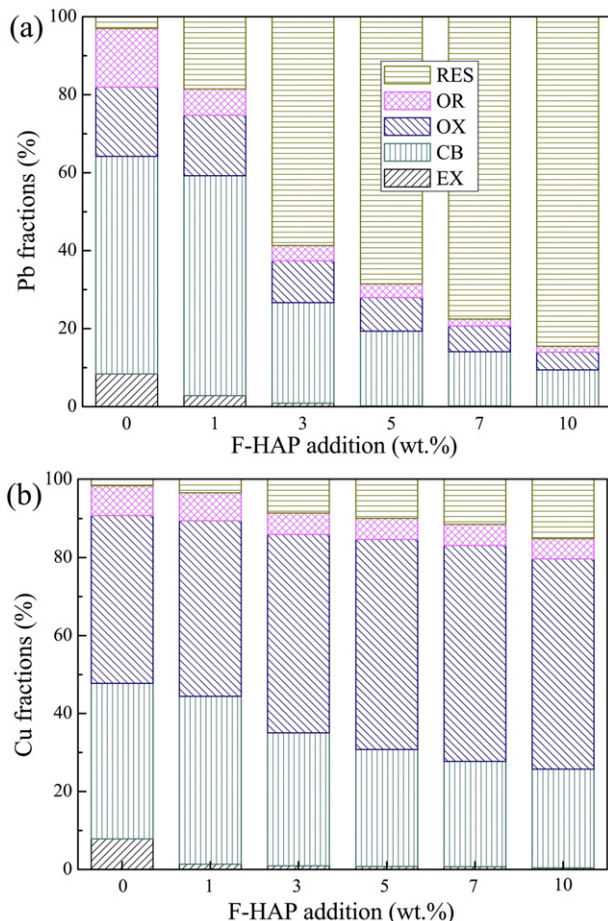
Langmuir, I., 1918. The adsorption of gases on plane surfaces of glass, mica and platinum. J. Am. Chem. Soc. 40, 1361–1368.

Lasheen, M.R., Ammar, N.S., Ibrahim, H.S., 2012. Adsorption/desorption of Cd(II), Cu(II) and Pb(II) using chemically modified orange peel: equilibrium and kinetic studies. Soild State Sci. 14, 202–210.

LeGeroes, R.Z., LeGeroes, J.P., 1984. In: Nriagu, J.O. (Ed.), Phosphate Minerals. Springer-Verlag, Berlin, pp. 351–385.

Li, Y.H., Di, Z., Wu, D., Luan, Z., Zhu, Y., 2005. Adsorption thermodynamic, kinetic and de-sorption studies of Pb^{2+} on carbon nanotubes. Water Res. 39, 605–609.

Liang, W., Zhan, L., Piao, L., Rüssel, C., 2011. Lead and copper removal from aqueous solutions by porous glass derived calcium hydroxyapatite. Mater. Sci. Eng. B 176, 1010–1014.

Liu, R., Zhao, D., 2007. In situ immobilization of Cu(II) in soils using a new class of iron phosphate nanoparticles. Chemosphere 68, 1867–1876.

Liu, C., Bai, R., Ly, Q.S., 2008. Selective removal of copper and lead ions by diethylenetriamine-functionalized adsorbent: behaviors and mechanisms. Water Res. 42, 1511–1522.

Lu, R.K., 1999. Soil and Agro-Chemical Analysis Methods. Agricultural Science and Tech-nology Press, Beijing, China.

Ma, S., Zhang, J., Sun, D., Liu, G., 2015. Surface complexation modeling calculation of Pb(II) adsorption onto the calcined diatomite. Appl. Surf. Sci. 359, 48–54.

Matusik, J., Bajda, T., Manecki, M., 2008. Immobilization of aqueous cadmium by addition of phosphates. J. Hazard. Mater. 152, 1332–1339.

Meitei, M.D., Prasad, M.N.V., 2014. Adsorption of Cu(II), Mn(II) and Zn(II) by *Spirodela polyrhiza* (L.) Schleiden: equilibrium, kinetic and thermodynamic studies. Ecol. Eng. 71, 308–317.

Mignardi, S., Corami, A., Ferrini, V., 2012. Evaluation of the effectiveness of phosphate treatment for the remediation of mine waste soils contaminated with Cd, Cu, Pb, and Zn. Chemosphere 86, 354–360.

Muhammad, N., Gao, Y., Iqbal, F., Ahmad, P., Ge, R., Nishan, U., Rahim, A., Gonfa, G., Ullah, Z., 2016. Extraction of biocompatible hydroxyapatite from fish scales using novel ap-proach of ionic liquid pretreatment. Sep. Purif. Technol. 161, 129–135.

Ogawa, S., Katoh, M., Sato, T., 2015. Simultaneous lead and antimony immobilization in shooting range soil by a combined application of hydroxyapatite and ferrihydrite. En-viron. Technol. 36, 2647–2656.

Pawar, R.R., Lalhmunsiama, B., H.C., Lee, S.M., 2016. Activated bentonite as a low-cost ad-sorbent for the removal of Cu(II) and Pb(II) from aqueous solutions: batch and col-umn studies. J. Ind. Eng. Chem. 34, 213–223.

Piccirillo, C., Pereira, S.I.A., Marques, A.P.G.C., Pullar, R.C., Tobaldi, D.M., Pintado, M.E., Castro, P.M.L., 2013. Bacteria immobilisation on hydroxyapatite surface for heavy metals removal. J. Environ. Manag. 121, 87–95.

Rehman, H., Shakirullah, A.I., Hameedullah, S.S., 2006. Sorption studies of nickel ions onto sawdust of *Dalbergia sissoo*. J. Chin. Chem. Soc. 53, 1045–1052.

Sanosh, K.P., Chu, M.C., Balakrishnan, A., Kim, T.N., Cho, S.J., 2009. Utilization of biowaste eggshells to synthesize nanocrystalline hydroxyapatite powders. Mater. Lett. 63, 2100–2102.

Šćiban, M., Klasnja, M., Škrbić, B., 2006. Modified softwood sawdust as adsorbent of heavy metal ions from water. J. Hazard. Mater. 136, 266–271.

Seshadri, B., Bolan, N.S., Wijesekara, H., Kunhikrishnan, A., Thangarajan, R., Qi, F., Matheyarasu, R., Rocco, C., Mbene, K., Naidu, R., 2016. Phosphorus-cadmium interac-tions in paddy soils. Geoderma 270, 43–59.

Shahat, A., Awual, M.R., Khaleque, M.A., Alam, M.Z., Naushad, M., Chowdhury, A.M.S., 2015. Large-pore diameter nano-adsorbent and its application for rapid lead(II) de-tection and removal from aqueous media. Chem. Eng. J. 273, 286–295.

Suzuki, T., Ishiqaki, K., Miyake, M., 1984. Synthetic hydroxyapatites as inorganic cation ex-changers. Part 3: exchange characteristics of lead ions (Pb^{2+}). J. Chem. Soc. Faraday Trans. 1 (80), 3157–3165.

Tessier, A., Campbell, P.G.C., Bisson, M., 1979. Sequential extraction procedure for the spe-ciation of particulate trace metals. Anal. Chem. 51, 844–851.

USEPA, 1994. Technical Assistance Document for Completing With the TC Rule and Implementing the Toxicity Characteristic Leaching Procedure (TCLP). United States Environmental Protection Agency, New York.

Vila, M., Sandra Sánchez-Salcedo, S., Vallet-Regí, M., 2012. Hydroxyapatite foams for the immobilization of heavy metals: from waters to the human body. Inorg. Chim. Acta 393, 24–35.

Wang, Z., Nie, E., Li, J., Yang, M., Zhao, Y., Luo, X., Zheng, Z., 2012. Equilibrium and kinetics of adsorption of phosphate onto iron-doped activated carbon. Environ. Sci. Pollut. Res. 19, 2908–2917.

Wang, L., Yang, L., Li, Y., Zhang, Y., Ma, X., Ye, Z., 2010. Study on adsorption mechanism of Pb(II) and Cu(II) in aqueous solution using PS-EDTA resin. Chem. Eng. J. 163, 364–372.

Yan, M., Li, Z., 2016. Microwave-assisted functionalized lignin with dithiocarbamate for enhancing adsorption of Pb(II). Mater. Lett. 170, 135–138.

Yan, Y.B., Dong, X.L., Sun, X.L., Sun, X.Y., Li, J.S., Shen, J.Y., Han, W.Q., Liu, X.D., Wang, L.J., 2014. Conversion of waste FGD gypsum into hydroxyapatite for removal of Pb^{2+} and Cd^{2+} from wastewater. J. Colloid Interface Sci. 429, 68–76.

Yang, J., Mosby, D., 2006. Field assessment of treatment efficacy by three methods of phosphoric acid application in lead-contaminated urban soil. Sci. Total Environ. 366, 136–142.

Yang, G., Tang, L., Lei, X., Zeng, G., Cai, Y., Wei, X., Zhou, Y., Li, S., Fang, Y., Zhang, Y., 2014. Cd(II) removal from aqueous solution by adsorption on α-ketoglutaric acid-modified magnetic chitosan. Appl. Surf. Sci. 292, 710–716.

Zhang, M., 2011. Adsorption study of Pb(II), Cu(II) and Zn(II) from simulated acid mine drainage using dairy manure compost. Chem. Eng. J. 172, 361–368.

Zhang, Z., Li, M., Chen, W., Zhu, S., Liu, N., Zhu, L., 2010. Immobilization of lead and cadmi-um from aqueous solution and contaminated sediment using nano-hydroxyapatite. Environ. Pollut. 158, 514–519.

Zhang, D., Luo, H., Zheng, L., Wang, K., Li, H., Wang, Y., Feng, H., 2012. Utilization of waste phosphogypsum to prepare hydroxylapatite nanoparticles and its application to-wards removal of fluoride from aqueous solution. J. Hazard. Mater. 241/242, 418–426.

Zhu, Y., Hu, J., Wang, J., 2012. Competitive adsorption of Pb(II), Cu(II) and Zn(II) onto xan-thate-modified magnetic chitosan. J. Hazard. Mater. 221-222, 155–161.